Robotica (2017) volume 35, pp. 569–587. © Cambridge University Press 2015
doi:10.1017/S0263574715000715

Optimal gait planning for humanoids with 3D structure walking on slippery surfaces

Majid Khadiv†*, S. Ali A. Moosavian†, Aghil Yousefi-Koma‡, Majid Sadedel‡ and Saeed Mansouri§

†*Center of Excellence in Robotics and Control, Advanced Robotics & Automated Systems (ARAS) Lab, Department of Mechanical Engineering, K. N. Toosi University of Technology, Tehran, Iran*
‡*Center of Advanced Systems and Technologies (CAST), School of Mechanical Engineering, College of Engineering, University of Tehran, Tehran, Iran*
§*Department of Mechanical Engineering, Sharif University of Technology, Tehran, Iran*

(Accepted July 23, 2015. First published online: September 1, 2015)

SUMMARY
In this study, a gait optimization routine is developed to generate walking patterns which demand the lowest friction forces for implementation. The aim of this research is to fully address the question "which walking pattern demands the lowest coefficient of friction amongst all feasible patterns?". To this end, first, the kinematic structure of the considered 31 DOF (Degrees of Freedom) humanoid robot is investigated and a closed-form dynamics model for its lower-body is developed. Then, the medium through which the walking pattern generation is conducted is presented. In this medium, after designing trajectories for the feet and the pelvis, the joint space variables are obtained, using the inverse kinematics. Finally, by employing a genetic algorithm (GA), an optimization process is conducted to generate walking patterns with the minimum Required Coefficient Of Friction (RCOF). Six parameters are adopted to parameterize the pelvis trajectory and are exploited as the design variables in this optimization procedure. Also, a parametrical study is accomplished to address the effects of some other variables on RCOF. For comparison purposes, a tip-over Stability Margin (SM) is defined, and an optimization procedure is conducted to maximize this margin. Finally, the proposed gait planning procedure is implemented on SURENA III, a humanoid robot designed and fabricated in CAST, to validate the developed simulation procedure. The obtained results reveal merits of the proposed optimal gait planning procedure in terms of RCOF.

KEYWORDS: Humanoid robots; Bipedal walking; Gait optimization; Walking on slippery surfaces.

Nomenclature

DOF	Degree of Freedom
RCOF	Required Coefficient of Friction
GA	Genetic Algorithm
SM	Stability Margin
ZMP	Zero Moment Point
SP	Support Polygon
COM	Center of Mass
SSP	Single Support Phase
DSP	Double Support Phase
t	Time
$q = \begin{bmatrix} q_p & q_r & q_l \end{bmatrix}^T$	Vector of generalized coordinates

* Corresponding author. E-mail: mkhadiv@mail.kntu.ac.ir

https://doi.org/10.1017/S0263574715000715 Published online by Cambridge University Press

$\boldsymbol{M}(\boldsymbol{q})$	Generalized mass matrix
$\boldsymbol{V}(\boldsymbol{q}, \dot{\boldsymbol{q}})$	Vector of coriolis, gyration and centrifugal effects
$\boldsymbol{G}(\boldsymbol{q})$	Vector of gravitational effects
$\boldsymbol{Q}$	Generalized force vector
$\boldsymbol{B}$	Matrix of actuating torque selection
$\boldsymbol{\tau}$	Actuating joint torques vector
$\boldsymbol{N}$	Number of contact points
$\boldsymbol{J}(\boldsymbol{q})$	Jacobian matrix
$\boldsymbol{F} = \left[\boldsymbol{f}_x, \boldsymbol{f}_y, \boldsymbol{f}_z, \boldsymbol{M}_x, \boldsymbol{M}_y, \boldsymbol{M}_z\right]^T$	Interaction force and moment vector
$\boldsymbol{I}$	Identity matrix
$\boldsymbol{k}$	Arbitrary constant
$\boldsymbol{0}$	Zero matrix
$\boldsymbol{\mu}_{\text{req}}$	Required coefficient of friction
$\boldsymbol{d}_{\text{ZMP}} = [\boldsymbol{x}_{\text{ZMP}}, \boldsymbol{y}_{\text{ZMP}}]$	Vector of ZMP components
$\left[\boldsymbol{x}_{\text{ZMP,ref}}, \boldsymbol{y}_{\text{ZMP,ref}}\right]$	Vector of reference ZMP components
$\boldsymbol{E}_{\text{ZMP}}$	Distance between ZMP and reference ZMP
$\boldsymbol{Z}_{\min}$	Minimum pelvis height
$\boldsymbol{Z}_{\max}$	Maximum pelvis height
$\boldsymbol{x}_s$	Sagittal distance between the pelvis and the support foot at the start of SSP
$\boldsymbol{x}_e$	Sagittal distance between the pelvis and the support foot at the end of SSP
$\boldsymbol{y}_d$	Lateral distance between the pelvis reference point and the inertial coordinate origin at the start of SSP
$\boldsymbol{y}_m$	Lateral distance between the pelvis reference point and the inertial coordinate origin at the mid-time of SSP
$\boldsymbol{L}_p$	Pelvis length
$\boldsymbol{D}_S$	Step length
$\boldsymbol{T}_S$	SSP time period
$\boldsymbol{T}_d$	DSP time period
$\boldsymbol{T}_c$	Walking step time period
$\boldsymbol{X}_{rf} = \left[\boldsymbol{x}_{rf}, \boldsymbol{y}_{rf}, \boldsymbol{z}_{rf}, \boldsymbol{\alpha}_{rf}, \boldsymbol{\beta}_{rf}, \boldsymbol{\gamma}_{rf}\right]^T$	Posture vector of the right foot reference point
$\boldsymbol{X}_{lf} = \left[\boldsymbol{x}_{lf}, \boldsymbol{y}_{lf}, \boldsymbol{z}_{lf}, \boldsymbol{\alpha}_{lf}, \boldsymbol{\beta}_{lf}, \boldsymbol{\gamma}_{lf}\right]^T$	Posture vector of the left foot reference point
$\boldsymbol{X}_p = [\boldsymbol{x}, \boldsymbol{y}, \boldsymbol{z}, \boldsymbol{\alpha}, \boldsymbol{\beta}, \boldsymbol{\gamma}]^T$	Posture vector of the pelvis reference point
$\boldsymbol{a}_0, \boldsymbol{a}_1, \ldots$	Polynomial coefficients of the trajectory
$\boldsymbol{b}_0, \boldsymbol{b}_1, \ldots$	Polynomial coefficients of the trajectory
$\boldsymbol{O}$	Objective function

1. Introduction

There always exist many patterns which may realize a specified walking gait for a humanoid robot, because of having so many DOF. However, due to the unilateral contact between the feet and the ground surface, only those patterns which satisfy the motion feasibility constraints can be realized. Hence, generating walking patterns which satisfy the feasibility constraints, and also are optimal in terms of expected performance indices have been of great interest in the humanoid robotics field.

In order to generate feasible gaits, some researchers exploited a full dynamics model of the robot in the process of gait planning to optimize the motion based on some dynamic-based performance criteria i.e. energy consumption,[1,2] joints actuating torque.[2–4] The full dynamics model has been used by these works to satisfy the constraints imposed due to the unilateral contact between the feet and the ground surface by considering the inequality constraints.[5] Instead, many other researchers adopted ground reference points to satisfy feasibility constraints. Although there have been proposed some ground reference points for the motion feasibility analyses of biped robots,[6,7] the most well-known and intuitive one is certainly the Zero Moment Point (ZMP) which was introduced by Vukobratovic.[8,9] ZMP represents a point on the ground about which the horizontal interaction

https://doi.org/10.1017/S0263574715000715 Published online by Cambridge University Press

moments become zero. Provided that the ZMP locates inside the Support Polygon (SP), the stance foot (feet) would not rotate around the edges of SP.

To generate feasible walking patterns employing ZMP, typically two approaches have been adopted. The first approach uses a simple inverted pendulum model to generate real-time walking patterns.[10–12] However, the second approach exploits the actual mass properties of each link, i.e. Center of Mass (COM) location, as well as mass and moment of inertia to generate offline walking patterns. So, the second approach uses a complete model with precise values of the parameters, and the exact location of ZMP will be computed which makes this method suitable for generating optimal walking patterns. Employing this method, Huang *et al*. stated the problem of gait planning as searching through hip motions and finding the pattern which provides the maximum SM.[13] Dau *et al*. parameterized the hip and the feet trajectories to generate energy-efficient motions.[14] Also, Capi *et al*. proposed a gait optimization procedure using GA to minimize energy consumption as well as torque fluctuation during walking on flat terrain and walking up stairs.[15] Park *et al*. optimized the energy consumption of a seven-link biped robot in the sagittal plane and analyzed the best location for COM of the links.[16] In the ZMP-based gait planning paradigm, it is assumed that the no-slip constraints are preliminarily fulfilled. In fact, the friction coefficient between the feet and the ground surface is assumed to be sufficient. However, in order to walk on the slippery surfaces or walk with relatively high speeds, this assumption may be violated.

Slippage is a hazardous phenomenon not only for biped robots, but for human beings. Due to the significance of investigating slippage during walking, many research studies have been carried out in the field of biomechanics to examine effects of various parameters of human walking on slippery surfaces. Most of these studies have focused on the effects of prior knowledge on the adaptations that old and young subjects employ to prevent slipping while walking on slippery surfaces.[17–21] In these studies, it has been observed that human beings change the gait parameters in the case of anticipating slippery situations to reduce the friction forces and possibility of slippage occurrence. Furthermore, some researchers have addressed parameters that may be employed to predict slippage phenomenon,[22] as well as measuring these parameters[23] for human walking.

The research studies that have been carried out focusing on slippage effects (as a destabilizing phenomenon) of bipedal walking can be divided into three categories. The first category deals with estimation of the friction coefficient between the feet and the ground surface during walking, and detection of slippage occurrence. The second category consists of research studies that have been done concentrating on generating walking patterns which are suitable for implementation on slippery terrains. The last category is dedicated to the reflexive actions that may be used to prevent falling in the case of feet slippage.

The first step in gait planning for walking on slippery surfaces and exploiting suitable reflexive actions in the case of slippage is estimation of the friction coefficient between the feet and the ground surface, and slippage detection. Yamamoto *et al*. used accelerometers on the robot feet to detect slippage of the stance foot.[24] Based on their algorithm, if acceleration of the stance foot exceeds zero, the stance foot would tend to slip. Kaneko *et al*. introduced a slip-observer to detect slippage of the stance foot.[25] Based on their medium, the difference between the actual horizontal forces which are measured using the embedded sensors, and the desired horizontal forces obtained from the pendulum model yields the slip forces. Hashlamon *et al*. adopted the same approach and developed the Virtual slip Force Sensor (VSFS).[26] In these research studies, the slippage is detected, only after it occurs. However, in order to generate walking patterns consistent with the surface that the robot walks on, the friction coefficient should be estimated before slipping. Hence, Roosen proposed an algorithm for estimation of the friction coefficient between the robot feet and the ground surface.[27] In this study, a first-order Bliman–Sorine friction model[28] has been used and a method based on the recursive least squares has been adopted to estimate the friction coefficient between the feet and the ground surface.

The frictional constraints imposed on the bipedal robots walking can be separated into the interacting yaw moment and the horizontal forces which should be restricted to a certain region to guarantee the feasibility of motion. In this notion, Zhou *et al*. have fully addressed the frictional constraints in biped walking. They showed that in some cases slippage due to rotation is more crucial than translation.[29] In order to reduce the possibility of rotational slipping due to the yaw moment interaction, some strategies based on trunk rotation and arms swinging have been proposed which are known as the yaw moment compensation.[30,31] Referring to these strategies, by using suitable arms and trunk motion, the interacting yaw moment can be regulated. On the other hand, since

https://doi.org/10.1017/S0263574715000715 Published online by Cambridge University Press

the rotation of trunk and arms about the vertical axis do not affect the COM motion (due to the upper-body symmetry), these motions directly affect the yaw moment interaction, independent of other interacting components. However, the translational slippage avoidance should be taken into consideration during pattern synthesis for the lower-body. To do so, Kajita *et al*. used the preview control to generate walking patterns which are suitable for slippery surfaces.[32] They also presented the slip-concerned ZMP equations to predict falling due to slipping. Furthermore, Brandao *et al*. proposed a gait planning approach which optimizes the motion speed in existence of the frictional constraints.[33] They adopted their method for both bent-knee and stretched-knee walking patterns.

Though the slippage prevention algorithms may reduce the possibility of slippage occurrence, they cannot guarantee that the robot can walk on the slippery surfaces without slipping. The reason is that in the process of implementing the walking patterns in reality, there exist some uncertainties and disturbances which may cause slippage. As a result, some strategies should be considered to recover posture of the robot, in the case of slipping. Boone *et al*. addressed these strategies as reflexive actions which are done based on the sensory information and without explicitly modeling the phenomenon.[34] Their strategies were based on increasing the vertical interaction force using the hip joint torque, and landing the swing foot for recovery purposes. Kwon *et al*. divided their strategies into detection, adaptation, and recovery phases.[35] They used upper-body vertical acceleration to increase the vertical interacting force, swing leg motion to reduce the destabilizing moment, and upper-body horizontal acceleration for control of ZMP. Furthermore, Kaneko *et al*. used their proposed slip-observer to reduce the upper-body roll due to slip, by estimating destabilizing moment on the torso.[25]

Certainly, the best option to circumvent slipping phenomenon during walking is to exploit walking patterns consistent with the friction coefficient between the feet and the ground surface. In order to walk on slippery surfaces, the walking patterns should demand low friction coefficient. So, in this paper, we aim at finding the pattern with the minimum RCOF, among all feasible walking patterns with the same gait characteristics. To do so, a gait planning paradigm based on a comprehensive model of the robot will be developed. By taking into account of the pelvis trajectory parameters as the design variables, a GA-based optimization procedure will be carried out to find the walking pattern which is suitable for implementation on slippery surfaces. Furthermore, the obtained results will be compared to the walking patterns which provide the maximum SM. More specifically, in this paper we extract the extremes of the spectrum of the feasible interacting forces and moments, for various walking speeds. These values provide a database for the high-level control unit to check whether or not there exists a feasible walking pattern for a specified walking speed and surface characterization. In the case that there is no solution, the waking speed should be reduced, by the gait coordinator, to a feasible walking pattern can be found. The rest of this paper is as follows: in Section 2, a comprehensive dynamics model for the lower-body of the robot is developed. Section 3 describes the gait planning procedure and formulating the optimization problem. Section 4 is dedicated to the results and discussions. Finally, Section 5 presents the concluding remarks.

2. Dynamics Modeling

The humanoid robot SURENA III (Fig. 1) is composed of 12 DOF in its lower-body and 19 DOF in its upper-body. This robot has 6 DOF in each leg (3 DOF for hip, 1 DOF for knee, 2 DOF for ankle), 7 DOF in each arm (3 DOF for shoulder, 1 DOF for elbow, 3 DOF for wrist), 1 DOF in each hand (a simple gripper), one DOF in its torso and 2 DOF in its neck. In this study, in order to investigate bipedal walking of this robot, upper-body joints are considered to be fixed and the whole upper-body is modeled with a single rigid body. So, in this section, a closed-form dynamics model for a bipedal robot with 12 active DOF will be developed. The procedure of dynamics model development for the robot with upper-body joints has been fully addressed by the authors.[36]

The vector of generalized coordinates which describes motion of the bipedal robot may be stated as

$$q = \begin{bmatrix} q_p & q_r & q_l \end{bmatrix}^T, \tag{1}$$

where q_p is a vector with six elements which describes motion of the pelvis with respect to the inertial coordinate system. Also, q_r and q_l are six-dimensional vectors which represent joint angles of the right leg and the left leg, respectively. The general form of dynamics model of the robot may be stated

https://doi.org/10.1017/S0263574715000715 Published online by Cambridge University Press

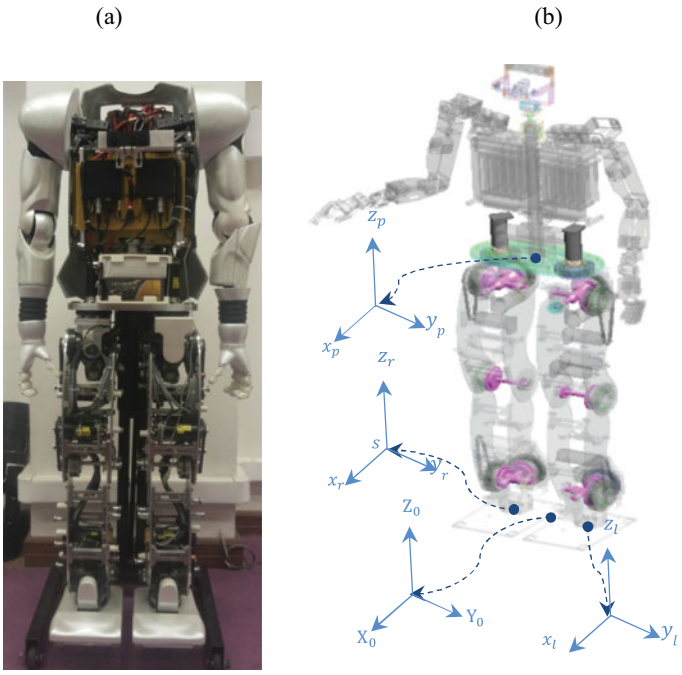


Fig. 1. SURENA III, a humanoid robot designed and fabricated in CAST, University of Tehran, (a) Real photo, (b) Developed model.

as

$$M(q)\ddot{q} + V(q, \dot{q}) + G(q) = Q. \tag{2}$$

The first term in the left-hand side of this equation represents the inertial effects, the second term groups together the centrifugal and Coriolis and gyration effects, and the third term specifies the gravitational effects. Each term yields a vector with 18 elements. The right-hand side of this equation is the generalized force vector which is projection of the joint actuating torques and interacting forces and moments to the space of generalized coordinates. This vector can be stated in a general form as

$$Q = B\tau + \sum_{i=1}^{N} J_i^T F_i. \tag{3}$$

In this equation, B is a selection matrix which maps the effects of joint actuating torques to the space of generalized coordinates. Since the relative joint angles of the legs are considered as generalized coordinates in this study, vector B may be related as

$$B = \begin{bmatrix} 0_{12\times 6} & I_{12\times 12} \end{bmatrix}^T. \tag{4}$$

Also, τ is a 12-dimensional vector of actuating torques, J is the Jacobian matrix of the contact points, and F is the vector of interacting components. Also, N specifies the number of robot-environment interaction points. This value varies during different phases of walking, i.e. the Single Support Phase (SSP) and the Double Support Phase (DSP). During SSP, one of the feet is fixed to the ground surface and the other one swings on a desired trajectory. Without loss of generality, assume the right foot interacts with the ground surface and the left foot has no interaction with the environment, in this phase (as it is illustrated in Fig. 2). Hence, the generalized force vector is

$$Q = B\tau + J_{r,s}^T F_{r,s}, \tag{5}$$

https://doi.org/10.1017/S0263574715000715 Published online by Cambridge University Press

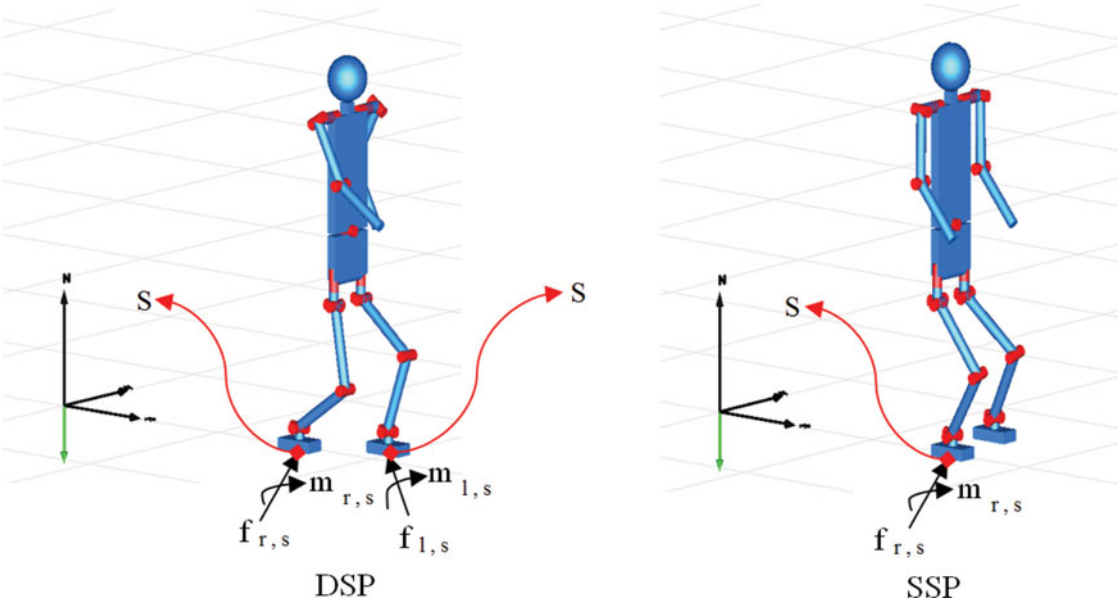


Fig. 2. Interaction forces and moments exerted from the ground surface to the feet during SSP and DSP.

where index r specifies the right leg. Furthermore, s is an arbitrary point on the interacting surface which is considered to be the point under the ankle joints intersection as the center of foot coordinate system (Figs. 1 and 2), in this study. Also, $J_{r,s}$ is a 6×18 matrix which specifies Jacobian of the point s, and $F_{r,s}$ is a six-dimensional vector which represents interacting forces and moments. Substituting Eqs. (5) and (4) into Eq. (2) and manipulating the result yields:

$$M(q)\ddot{q} + V(q,\dot{q}) + G(q) = \begin{bmatrix} B & J_{r,s}^T \end{bmatrix} \begin{bmatrix} \tau \\ F_{r,s} \end{bmatrix}, \tag{6}$$

where $[\, B \;\; J_{r,s}^T \,]$ is a square 18×18 matrix. As a result, this set of linear equations (for a specified walking pattern) may be solved for a unique solution of the actuating torques and interacting forces and moments (the matrix $\begin{bmatrix} B & J_{r,s}^T \end{bmatrix}$ is assumed to be invertible):

$$\begin{bmatrix} \tau \\ F_{r,s} \end{bmatrix} = \begin{bmatrix} B & J_{r,s}^T \end{bmatrix}^{-1} \left[M(q)\ddot{q} + V(q,\dot{q}) + G(q) \right]. \tag{7}$$

During DSP, both feet are fixed to the ground surface (Fig. 2). So, the matrix Q, in this case, can be stated as

$$Q = B\tau + J_{r,s}^T F_{r,s} + J_{l,s}^T F_{l,s}. \tag{8}$$

Again, by introducing Eqs. (8) and (4) into Eq. (2) and manipulating the result, we can relate this equation in a compact form as

$$M(q)\ddot{q} + V(q,\dot{q}) + G(q) = \begin{bmatrix} B & J_{r,s}^T & J_{l,s}^T \end{bmatrix} \begin{bmatrix} \tau \\ F_{r,s} \\ F_{l,s} \end{bmatrix}. \tag{9}$$

In this case, the matrix $[\, B \; J_{r,s}^T \; J_{l,s}^T \,]$ is a non-square 18×24 matrix. Hence, the set of Eq. (9) is under-determined. The reason is that in DSP the legs constitute a closed kinematic chain with the actuation redundancy. Consequently, the inverse dynamics problem has infinitely many solutions

https://doi.org/10.1017/S0263574715000715 Published online by Cambridge University Press

which may be represented as the following closed-form equation:

$$\begin{bmatrix} \tau \\ F_{r,s} \\ F_{l,s} \end{bmatrix} = \begin{bmatrix} B & J_{r,s}^T & J_{l,s}^T \end{bmatrix}^{\dagger} \left[M(q)\ddot{q} + V(q,\dot{q}) + G(q) \right] + \left(I - \begin{bmatrix} B & J_{r,s}^T & J_{l,s}^T \end{bmatrix}^{\dagger} \begin{bmatrix} B & J_{r,s}^T & J_{l,s}^T \end{bmatrix} \right) k. \tag{10}$$

where $[]^{\dagger}$ is Moore–Penrose inverse (Pseudo inverse), and k is an arbitrary constant. For each value of the constant k, one solution can be obtained. However, one interesting solution may be obtained when the value k is set to zero. In this case, the inverse dynamics solution would be

$$\begin{bmatrix} \tau \\ F_{r,s} \\ F_{l,s} \end{bmatrix} = \begin{bmatrix} B & J_{r,s}^T & J_{l,s}^T \end{bmatrix}^{\dagger} \left[M(q)\ddot{q} + V(q,\dot{q}) + G(q) \right]. \tag{11}$$

This solution set yields the minimum quadratic norm of the vector of the actuating torques and interacting forces and moments.

In order to realize a walking pattern, the interacting forces and moments should satisfy the motion feasibility constraints. To guarantee that the stance foot (feet) would not slip during motion, the friction coefficient between the feet and the ground surface should be lower than the maximum friction coefficient that the walking pattern demands. The RCOF can be obtained, using the following equations:

$$\mu_{\text{req}} = \frac{\sqrt{(f_{xl} + f_{xr})^2 + \left(f_{yl} + f_{yr}\right)^2}}{f_{zl} + f_{zr}}, \tag{12}$$

in which f_x and f_y are the horizontal interacting forces and f_z specifies vertical interacting force. Also, indices r and l stand for the right and left foot, respectively. μ_{req} is always positive and shows the amount which is required in order for a specified walking pattern to be realized. Furthermore, in order to examine the possibility of slippage occurrence in each sagittal and lateral direction, the components of RCOF in each direction may be defined:

$$\begin{cases} \mu_{x,\text{req}} = \dfrac{(f_{xl} + f_{xr})}{f_{zl} + f_{zr}} \\ \mu_{y,\text{req}} = \dfrac{\left(f_{yl} + f_{yr}\right)}{f_{zl} + f_{zr}} \end{cases} \tag{13}$$

In these equations, $\mu_{x,\text{req}}$ and $\mu_{y,\text{req}}$ specify RCOF in the sagittal and lateral directions, respectively. Although μ_{req} is a positive scalar value, $\mu_{x,\text{req}}$ and $\mu_{y,\text{req}}$ may have both positive and negative values which show the direction that the robot tends to slip. For instance, the positive or negative values of the $\mu_{x,\text{req}}$ show that the robot tends to slip backward or forward.

In order to guarantee the tip-over stability of the robot during walking, ZMP should be within SP. ZMP can be computed in terms of the interaction components, using the following equations:

$$\begin{cases} x_{\text{ZMP}} = \dfrac{f_{zl}x_{lf} + f_{zr}x_{rf} - M_{yl} - M_{yr}}{f_{zl} + f_{zr}} \\ y_{\text{ZMP}} = \dfrac{f_{zl}y_{lf} + f_{zr}y_{rf} + M_{xl} + M_{xr}}{f_{zl} + f_{zr}} \end{cases} \tag{14}$$

where M_x and M_y are interacting sagittal and lateral moments acting on the stance feet, respectively. Also, the vertical interacting forces should be positive to satisfy the unilateral constraints, during walking. These constraints will be taken into consideration during walking pattern generation, in the next section. Furthermore, the friction coefficient should be high enough to prevent rotation

https://doi.org/10.1017/S0263574715000715 Published online by Cambridge University Press

of the stance foot about the vertical axis. However, since the yaw moment that is generated due to the walking can be regulated by the trunk and arms motion,[31] independent of other constraints, this constraint may be ignored during pattern generation for the lower-body, in the rest of this paper.

3. Optimal Gait Planning

In this section, a gait planning routine in the task space will be fully described. As it is illustrated in Fig. 1, task space of the robot is composed of the feet and the pelvis to which coordinate systems are attached. In order to generate walking patterns suitable for various terrains, first, consistent with the surface on which the robot walks, the feet trajectories are designed. Then, the pelvis trajectory is generated to satisfy the feasibility constraints imposed due to the unilateral contact between the feet and the ground surface. Finally, by solving the inverse kinematics,[37] the desired joint trajectories may be obtained. Since there are many trajectories for the pelvis which satisfy the feasibility constraints, our interest is to find the pattern which demands the lowest friction coefficient amongst all feasible patterns. So, the problem of finding the lowest friction demanding pattern is formulated as an optimization procedure. Also, for Comparison purposes, an optimization procedure will be carried out to yield the pattern which provides the maximum SM.

3.1. Foot trajectory

The first step to generate walking patterns for bipedal robots is to design trajectories for the feet compatible with the surface that the robot walks on. As it is illustrated in Figs. 1 and 2, the coordinate systems are attached to the soles of the feet, on the point just under the intersection of the ankle joints. The trajectory generation for the feet is to plan motion of these coordinate systems with respect to the inertial coordinate system. So, for each foot, three components related to position of the origin of these coordinate systems and three components related to orientation of these coordinate systems should be generated.

For the sake of simplicity, the flat-feet walking is considered and the heel-off or toe-off motions are excluded from the feet patterns. Also, In order to avoid legs self-collision, the distance between the feet in the lateral direction is considered to be constant (Fig. 3). Based on these constraints, position of the feet in y-direction and all of the orientation components remain fixed during walking. During DSP and during SSP when the foot is the stance one, x and z components remain fixed, too. However, for the swing foot during SSP, the trajectories should be designed to not only satisfy the constraints consistent with the terrain that the robot walks on, but also fulfill the velocity and acceleration continuity conditions to generate C^2 smooth trajectories. The boundary conditions for posture of the feet during one gait cycle can be stated as

$$
\begin{cases}
x_{rf} = \begin{cases} 0, & 0 \le t \le T_d \\ 0 \to 2D_S, & T_d \le t \le T_c \\ 2D_S, & T_c \le t \le 2T_c \end{cases} \\
y_{rf} = 0, \quad 0 \le t \le 2T_c \\
z_{rf} = \begin{cases} 0, & 0 \le t \le T_d \\ 0 \to H_{\max}, & T_d \le t \le T_d + \frac{T_s}{2} \\ H_{\max} \to 0, & T_d + \frac{T_s}{2} \le t \le T_c \\ 0, & T_c \le t \le 2T_c \end{cases} \\
\alpha_{rf} = 0, \quad 0 \le t \le 2T_c \\
\beta_{rf} = 0, \quad 0 \le t \le 2T_c \\
\gamma_{rf} = 0, \quad 0 \le t \le 2T_c
\end{cases}
\quad
\begin{cases}
x_{lf} = \begin{cases} D_S, & 0 \le t \le T_d \\ D_S, & T_d \le t \le T_c + T_d \\ D_S \to 3D_S, & T_c + T_d \le t \le 2T_c \end{cases} \\
x_{lf} = L_p, \quad 0 \le t \le 2T_c \\
z_{lf} = \begin{cases} 0, & 0 \le t \le T_d \\ 0, & T_d \le t \le T_c + T_d \\ 0 \to H_{\max}, & T_c + T_d \le t \le T_c + T_d + \frac{T_s}{2} \\ H_{\max} \to 0, & T_c + T_d + \frac{T_s}{2} \le t \le 2T_c \end{cases} \\
\alpha_{lf} = 0, \quad 0 \le t \le 2T_c \\
\beta_{lf} = 0, \quad 0 \le t \le 2T_c \\
\gamma_{lf} = 0, \quad 0 \le t \le 2T_c
\end{cases}
\tag{15}
$$

In this equations, T_s, T_d, and T_c are the SSP, DSP and step period, respectively. Also, D_S and $H_{\max}$ are the step length and the maximum height of the swing foot which are illustrated in Fig. 3. Hence, for x-component of feet trajectories during the swing phase, a fifth order polynomial is considered to satisfy the position boundary conditions, and the velocity and acceleration continuity constraints. Similarly, in z-direction, a sixth order polynomial is adopted.

https://doi.org/10.1017/S0263574715000715 Published online by Cambridge University Press

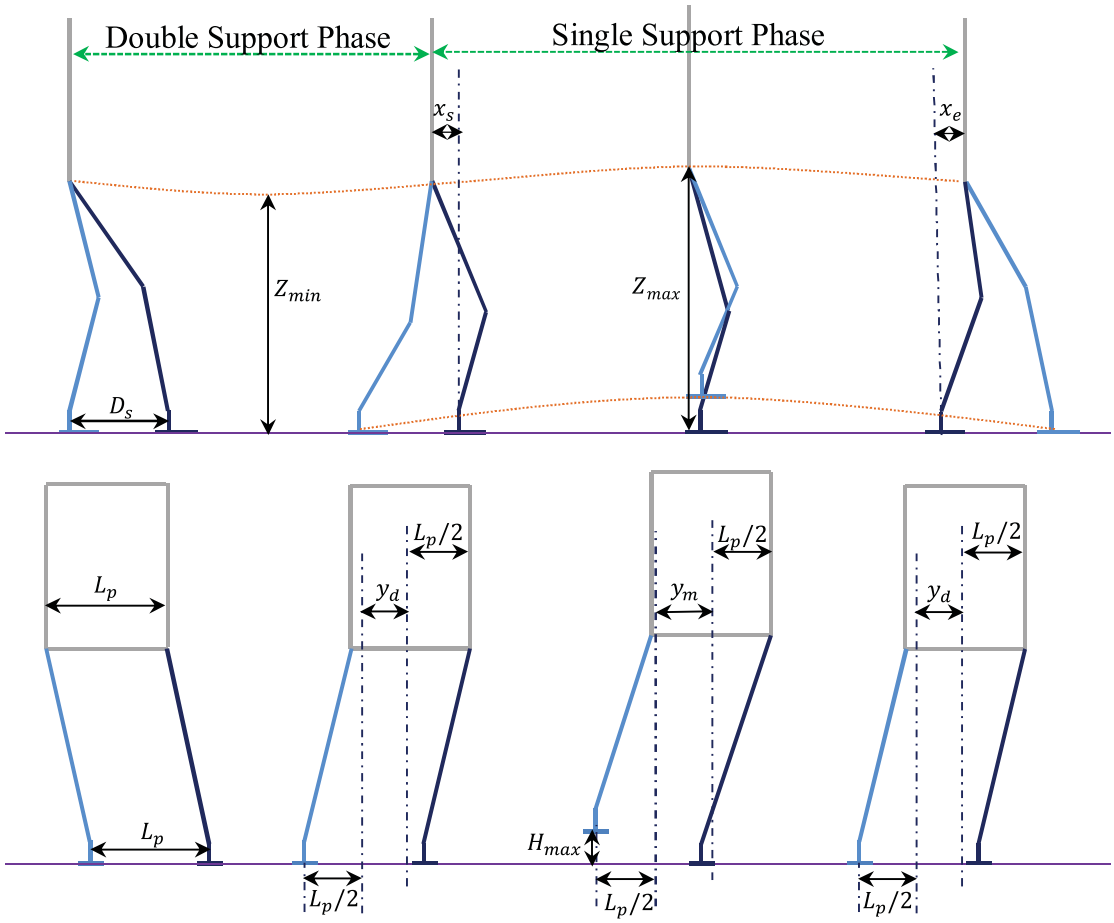


Fig. 3. Gait parameters specified in lateral and sagittal schematic views of walking.

3.2. Pelvis trajectory

After designing the feet trajectories for walking on a flat terrain, the pelvis trajectory should be generated such that satisfy the feasibility constraints. Since the upper-body joints are fixed during walking and there is no waist joint in the structure of the robot to move the trunk in the pitch and roll directions, it is desired to the upper-body remains in the upright posture during walking. So, the orientation components of the pelvis with respect to the inertial coordinate system are set to zero. However, for the pelvis reference point in three directions suitable trajectories should be designed.

For the sagittal direction, two parameters are exploited to formulize boundary conditions of the pelvis trajectory. x_s and x_e are two parameters which indicate the distance between the pelvis and the support foot in the first and last instances of SSP, as illustrated in Fig. 3. In general, there exist infinite numbers of values for these parameters. However, they should be selected such that not only satisfy the tip-over stability (ZMP should be within SP), but also minimize the fluctuations of the upper-body motion to minimize RCOF for walking on slippery surfaces. In the case that the tip-over stability is crucial, the acceleration in x-direction is needed to bring ZMP closer to the center of the stance foot, to provide satisfactory SM during SSP. This acceleration increases the demanded friction force for walking and as a result the RCOF and possibility of the slippage increases. To generate walking pattern which is suitable for implementation on slippery surfaces, the acceleration of the upper-body motion should be alleviated. A trivial case is when the step length is small and the step period is large.[38] In this case, the statically stable walking may be realized in which the acceleration of the upper-body is zero. In fact, the pelvis trajectory in x-direction would be a straight line during walking, while the pelvis and the ZMP trajectories coincide and both lie within SP. The parameters x_s and x_e, in this case, are both within SP and the pelvis trajectory is a line from x_e to $D_s - x_s$ during DSP, and from $D_s - x_s$ to $D_s + x_e$ during SSP. On the contrary, for walking with high speeds, it is not

https://doi.org/10.1017/S0263574715000715 Published online by Cambridge University Press

possible to generate statically stable walking and it is necessary to exploit upper-body acceleration to generate stable walking patterns. In this case, the less the acceleration on the upper-body is, the less the RCOF is. So, in general, the best trajectory for the pelvis with respect to the minimum RCOF is the one that relaxes the ZMP to graze around the SP boundaries and reduces the acceleration of the upper-body. In the next sections, the optimal patterns with the maximum SM and the minimum RCOF will be obtained and thoroughly discussed.

The trajectory for the pelvis should be C^2 smooth to not only generate continuous ZMP, but also yield desired smooth driving torques for the actuators. So, by considering two third-order polynomials for SSP and DSP, the coefficients may be computed to satisfy the position, velocity and acceleration constraints:

$$\begin{cases} x_{\mathrm{DSP}}(t) = a_0 + a_1 t + a_2 t^2 + a_3 t^3, \quad 0 \le t \le T_d \\ x_{\mathrm{DSP}}(0) = x_e, \quad x_{\mathrm{DSP}}(T_d) = D_s - x_s, \\ \dot{x}_{\mathrm{DSP}}(T_d) = \dot{x}_{\mathrm{SSP}}(T_d), \quad \ddot{x}_{\mathrm{DSP}}(T_d) = \ddot{x}_{\mathrm{SSP}}(T_d) \\ x_{\mathrm{SSP}}(t) = b_0 + b_1 t + b_2 t^2 + b_3 t^3, \quad T_d \le t \le T_c \\ x_{\mathrm{SSP}}(T_{d)} = D_s - x_s, \quad x_{\mathrm{SSP}}(T_c) = D_s + x_e, \\ \dot{x}_{\mathrm{DSP}}(0) = \dot{x}_{\mathrm{SSP}}(T_c), \quad \dot{x}_{\mathrm{DSP}}(0) = \dot{x}_{\mathrm{SSP}}(T_C) \end{cases} \tag{16}$$

For the lateral direction, also two parameters are considered as boundary conditions of the pelvis trajectory which are the lateral distance of the pelvis reference point with respect to the inertial coordinate system at the start and end of SSP (y_d), and at the mid-time of SSP (y_m), respectively. In Fig. 3, these parameters are specified. As a result, the considered polynomials and the boundary conditions may be stated as

$$\begin{cases} y_{\mathrm{DSP}}(t) = a_0 + a_1 t + a_2 t^2 + a_3 t^3, \quad 0 \le t \le T_d \\ y_{\mathrm{DSP}}(0) = -y_d, \quad y_{\mathrm{DSP}}(T_d) = y_d, \\ \dot{y}_{\mathrm{DSP}}(T_d) = \dot{y}_{\mathrm{SSP}}(T_d), \quad \ddot{y}_{\mathrm{DSP}}(T_d) = \ddot{y}_{\mathrm{SSP}}(T_d) \\ y_{\mathrm{SSP}}(t) = b_0 + b_1 t + b_2 t^2 + b_3 t^3 + b_4 t^4, \quad T_d \le t \le T_c \\ y_{\mathrm{SSP}}(T_d) = y_d, y_{\mathrm{SSP}}(T_d + T_s/2) = y_m, \quad y_{\mathrm{SSP}}(T_c) = y_d, \\ \dot{y}_{\mathrm{DSP}}(0) = \dot{y}_{\mathrm{SSP}}(T_c), \quad \ddot{y}_{\mathrm{DSP}}(0) = \ddot{y}_{\mathrm{SSP}}(T_c) \end{cases} \tag{17}$$

Finally, in the vertical direction, two parameters i.e. the maximum ($Z_{\max}$) and the minimum ($Z_{\min}$) height of the pelvis are adopted as the boundary conditions (Fig. 3). The robot is on its maximum height in the middle of SSP and on its minimum height in the middle of DSP. So, the trajectories in vertical direction would be

$$\begin{cases} z_1(t) = a_0 + a_1 t + a_2 t^2 + a_3 t^3, \quad \frac{T_d}{2} \le t \le T_d + \frac{T_s}{2} \\ z_1(T_d/2) = Z_{\min}, \quad z_1(T_d + T_s/2) = Z_{\max} \\ \dot{z}_1(T_d + T_s/2) = \dot{z}_2(T_d + T_s/2), \quad \ddot{z}_1(T_d + T_s/2) = \ddot{z}_2(T_d + T_s/2) \\ z_2(t) = b_0 + b_1 t + b_2 t^2 + b_3 t^3, \quad T_d + \frac{T_s}{2} \le t \le T_c + \frac{T_d}{2} \\ z_2(T_d + T_s/2) = Z_{\max}, \quad z_2(T_c + T_d/2) = Z_{\min} \\ \dot{z}_1(T_d/2) = \dot{z}_2(T_c + T_d/2), \quad \ddot{z}_1(T_d/2) = \ddot{z}_2(T_c + T_d/2) \end{cases} \tag{18}$$

Using Eqs. (16)–(18), the pelvis trajectory can be obtained and the procedure of gait planning would be completed. In these equations, six parameters should be specified to yield unique trajectory for the pelvis. Since the pelvis trajectory drastically affects the interacting forces, these parameters are exploited as the design variables for the optimization process.

3.3. Optimization procedure

After designing the task space trajectories for walking on flat surfaces, in this subsection, the optimization procedure for finding the walking pattern which demands the lowest friction coefficient among all feasible motions is described. Also, for comparison purposes, a procedure for optimizing the walking pattern for the maximum SM is adopted. It is noteworthy that it is highly desirable to design a walking pattern which considers both the tip-over stability and the slippage avoidance. So, it can be defined a multi-objective optimization problem to find a walking pattern which is optimal in terms of a weighted objective function which considers both matters and can be used in usual walking.

https://doi.org/10.1017/S0263574715000715 Published online by Cambridge University Press

However, it is of question, what the suitable weight would be. In fact, depending on the surface that the robot walks on and the slipperiness characterization of the surface, this weight should be selected. Furthermore, as it has been stated, the main aim of this paper is to address the desired interacting forces and moments between the feet and the ground surface during walking in critical situations. As a result, we extract the extremes of the spectrum of the feasible interacting forces and moments. So, the obtained walking patterns may be employed in critical situations whether the slippage avoidance or the tip-over stability is crucial.

As it was mentioned, since the interaction forces and moments depend on the pelvis motion, in order to generate feasible motion with the minimum RCOF, the pelvis parameters are considered as the design variables for the optimization. As defined in the last subsection, these parameters are

$$\text{Design Variables} = \left\{ x_s \quad x_e \quad y_d \quad y_m \quad z_{\min} \quad z_{\max} \right\}. \tag{19}$$

The objective function can be formulated as the maximum RCOF, during one walking step:

$$O_1 = \max \left\{ \mu_{\text{req}}(t) \right\}, \quad 0 \le t \le T_c, \tag{20}$$

in which $\mu_{\text{req}}(t)$ can be computed using Eq. (12). The goal of optimization is to find the walking pattern which minimizes the maximum RCOF for a walking step. The first constraint imposed on this problem is that the ZMP should lie inside SP:

$$d_{\text{ZMP}}(t) = [x_{\text{ZMP}}, y_{\text{ZMP}}] \in SP, \quad 0 \le t \le T_c \tag{21}$$

Also, in order to avoid singularity of the knee joint, its motion should be limited:

$$q_{\text{knee}}(t) > \varepsilon, \quad 0 \le t \le T_c \tag{22}$$

in which ε is a small positive constant. Finally, in order to check that the generated walking patterns are implementable, the actuating torques and the joint velocities for each leg should be consistent with the characteristics of the actuators:

$$\tau_i < \tau_{\max,i} \quad \text{and} \quad \dot{q}_i \le \dot{q}_{\max,i} \quad , i = 1, 2, \ldots, 6. \tag{23}$$

The optimization procedure is shown through an illustrative flowchart in Fig. 4. Also, in order to find walking pattern which provides the maximum SM, the objective function can be defined as the distance between the actual ZMP and the reference ZMP:

$$O_2 = \frac{1}{T_c} \int_0^{T_c} \sqrt{\left(x_{\text{ZMP}} - x_{\text{ZMP,ref}}\right)^2 + \left(y_{\text{ZMP}} - y_{\text{ZMP,ref}}\right)^2} dt, \tag{24}$$

in which $x_{\text{ZMP, ref}}$ and $y_{\text{ZMP, ref}}$ are illustrated in Fig. 9. The optimization procedure for finding motion with the maximum SM is illustrated in Fig. 4. In order to solve the optimization problem, the GA Toolbox in MATLAB is exploited and the obtained results will be discussed in the next section.

4. Results and Discussions

The mass properties and geometric attributes of the considered robot are specified in Table I. In order to verify the obtained results from the simulations, a walking pattern is implemented on the real robot and the obtained results are compared to the results obtained from dynamics model developed in the Section 2. Then, a comparison between motion with the minimum RCOF and motion with the maximum SM is made. Finally, a parametrical study is carried out to show the effects of some side parameters which are not included as the design variables during the optimization procedure.

4.1. Experimental and simulation results

The actuators of the considered humanoid robot in this study (SURENA III) are EC motors and the power transmission system is composed of the harmonic drive, and the timing-belt and pulley. Using

https://doi.org/10.1017/S0263574715000715 Published online by Cambridge University Press

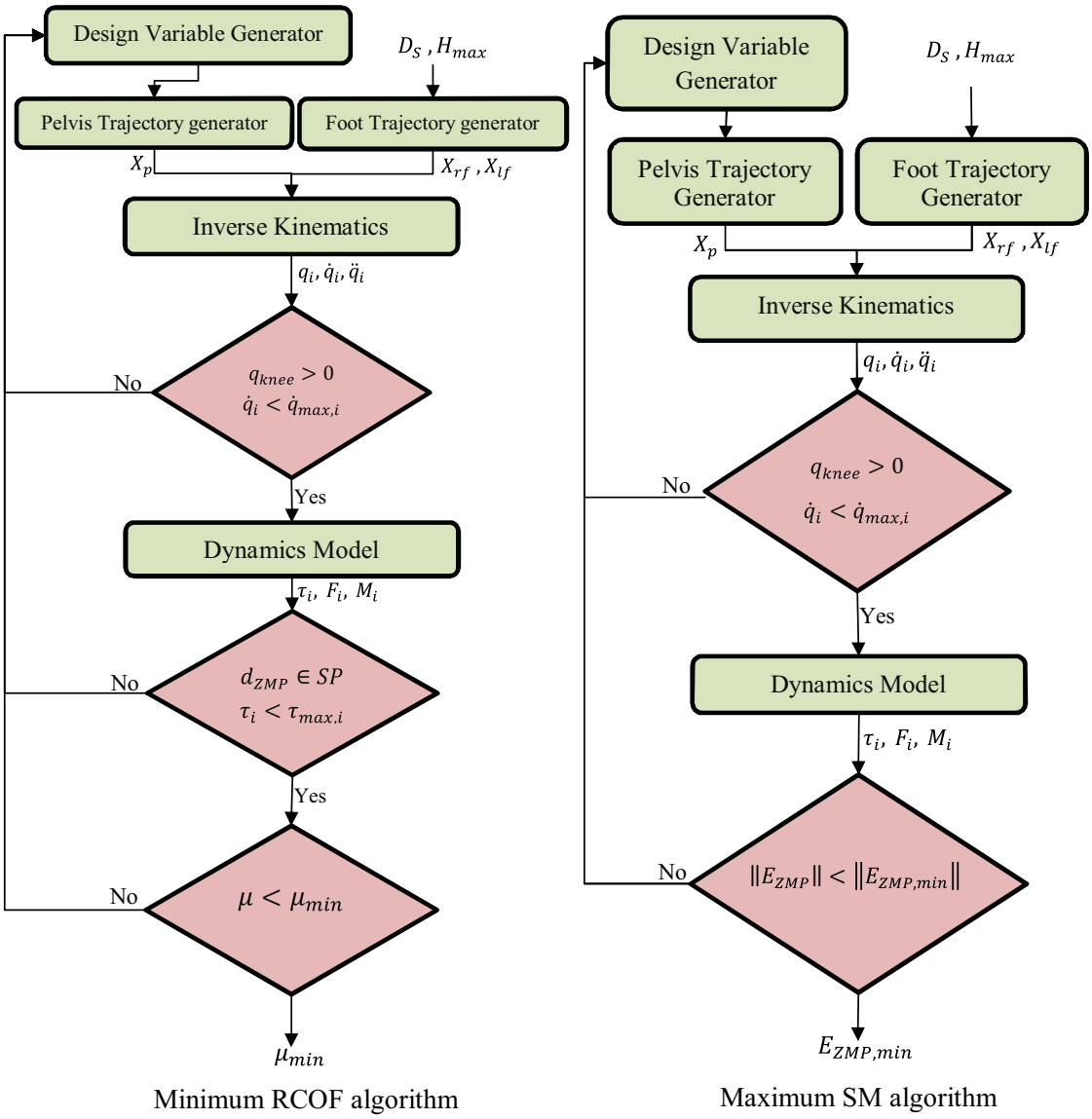


Fig. 4. Flowchart of the optimization procedure for both the Minimum RCOF and the Maximum SM algorithms.

the input current measured by the hall sensors that are embedded to the motors and multiplying it to the torque constant of the motor, the applied torque by the actuators may be computed. Finally, this value is multiplied to the gear ratio to yield the load-side torque. Also, six-axis F/T sensors are attached to the ankles to measure the interaction components. In order to verify the developed model in Section 2, the optimal walking pattern with the minimum RCOF and the speed of 0.5 Km/h is implemented on the robot and the simulation and experimental results are compared.

For the implemented walking pattern, the obtained interaction components from our dynamics model are compared to the measurements from F/T sensors during three successive gait cycles and the results are illustrated in Fig. 5. As it can be seen, the developed closed-form dynamics model (in Section 2) fairly models the behavior of the interaction between the feet and the ground surface. Although the measurements are in some stances different from the model in terms of quantity, the trends fairly match together. As it can be seen, the vertical component of the interaction forces is always positive which is consistent with the premise of the unilateral contact between the feet and the ground surface.

In Fig. 6, the applied torque by the actuators, obtained from the model and measured by the sensors, are illustrated. As it can be observed from these figures, the model fairly estimates the actuating torque

https://doi.org/10.1017/S0263574715000715 Published online by Cambridge University Press

Table I. Mass properties and geometric attributes of the under-study robot.

Link	Mass (gr)	Parameter	Value (mm)
Foot	3859	Foot length	265
Ankle	2236	Foot width	160
Shank	4561	Ankle joints height	98
Thigh	6327	Shank length	360
Pelvis	17800	Thigh length	360
Upper-body	28482	Distance between hip-rotation joints	230
Total weight: 82 (Kg)		Distance between hip and pelvis	115
		Distance between pelvis and head	767
		Total height: 1.85 (m)	

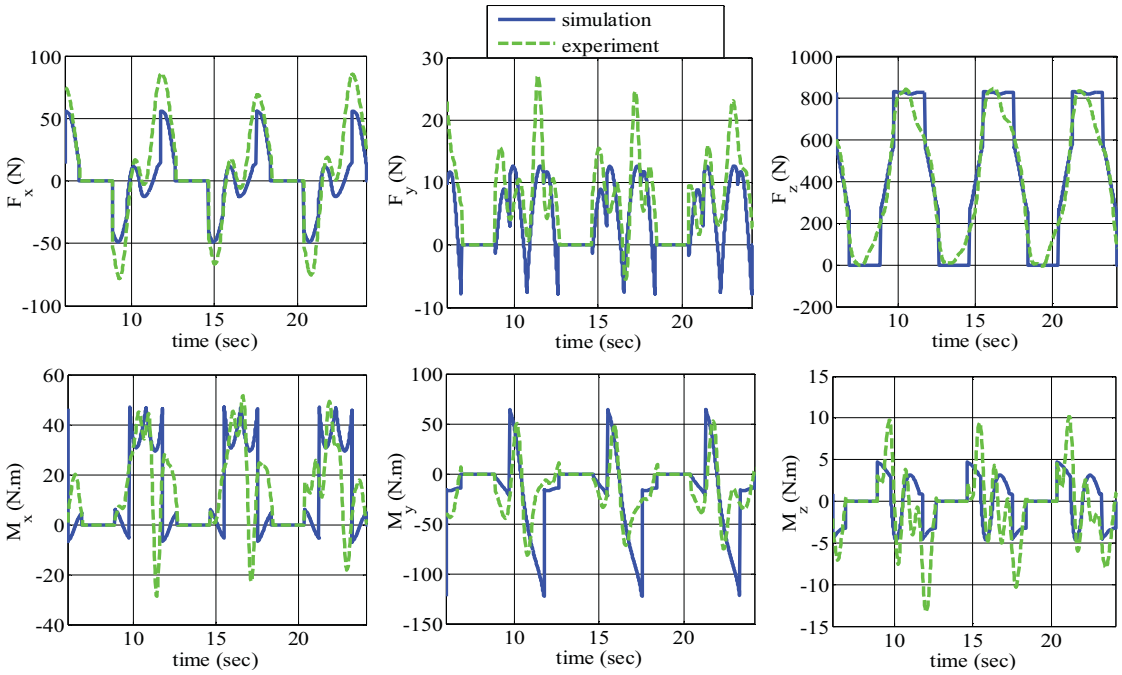


Fig. 5. Time history of interacting forces and moments of right foot for walking with speed of 0.5 Km/h during three gait cycles.

Table II. GA initial parameters for optimization.

Population size	Chromosome length	Crossover ratio	Initial population
100	6	0.8	[0.1 0.1 0.05 0.1 0.75 0.8]

required in order for the pattern to be realized. Furthermore, in Fig. 7 snapshots of the robot walking are shown which verify that the generated gaits are feasible.

4.2. Optimization results

In this subsection, characteristics of walking pattern with the minimum RCOF will be fully addressed and this walking pattern will be compared to that with the maximum SM. The results in this subsection are those obtained by optimizing the walking patterns with the speed of 1 Km/h and the step length of 40 cm. Also, ratio of the DSP time (T_d) to the step period (T_c) is set to 0.3. The effects of these parameters on the minimum RCOF will be discussed in the next subsection. In Table II, the GA parameters are specified. Furthermore, the obtained values of design variables and objective functions for optimal walking patterns are presented in Table III.

https://doi.org/10.1017/S0263574715000715 Published online by Cambridge University Press

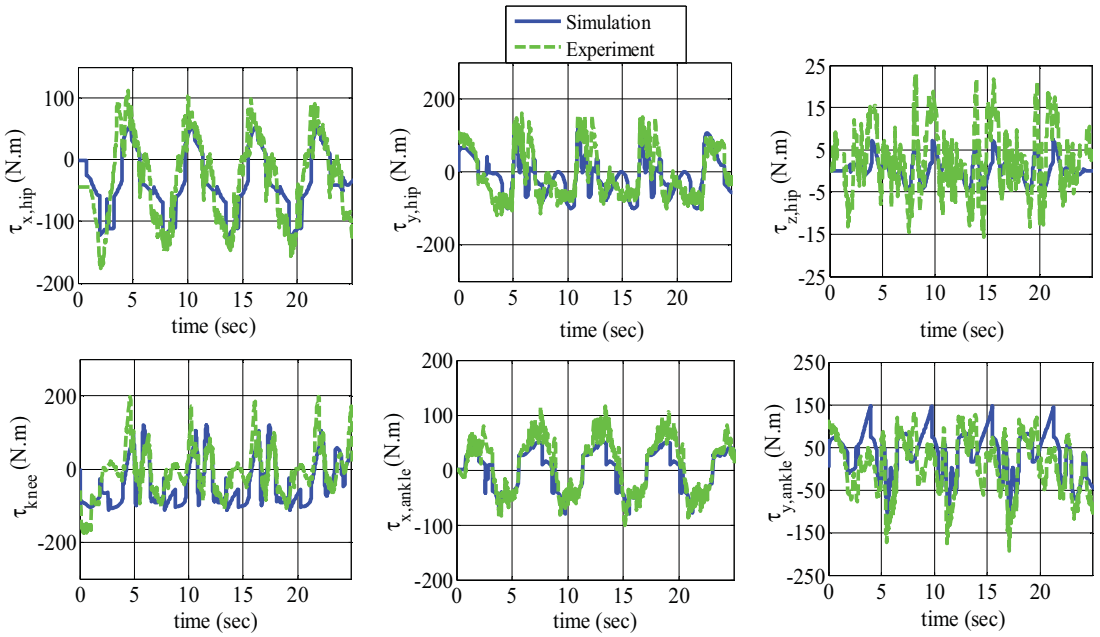


Fig. 6. Time history of actuating joints torques of right foot for walking with speed of 0.5 Km/h during three gait cycles.

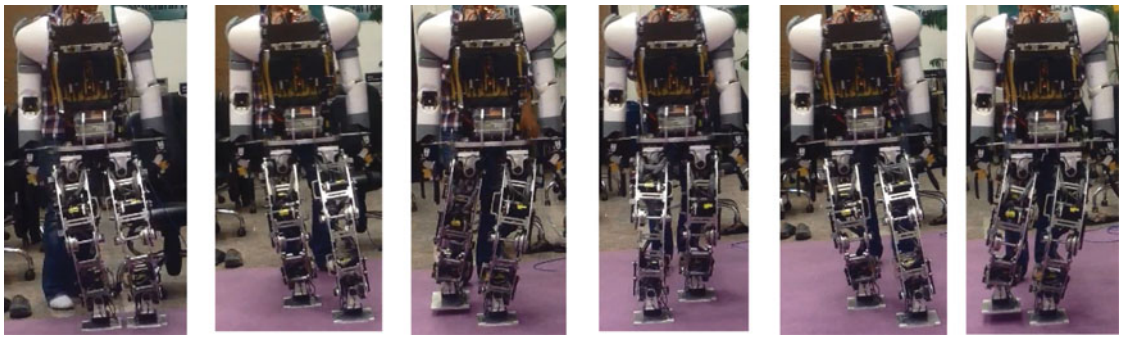


Fig. 7. Experimental validation of walking at 0.5 km/h. Snapshots are taken for one walking cycle. (SURENA III humanoid robot which is designed and fabricated in CAST, University of Tehran).

Table III. Design variables and objective functions values for optimal walking patterns.

Method	x_e	x_s	y_d	y_m	$z_{\min}$	$z_{\max}$	Objective function
Max. SM	0.0914	0.0733	0.0526	0.0950	0.7518	0.8017	0.1088
Min. RCOF	0.1084	0.1118	0.0449	0.0901	0.7818	0.8018	0.0661

In Fig. 8, components of the pelvis trajectory for both cases during one gait cycle are plotted. As it can be observed in these figures, the fluctuations of pattern with the minimum RCOF are less than those with the maximum stability. The reason is that in order to alleviate the horizontal interacting forces, the upper-body horizontal accelerations should be reduced. Hence, the fluctuations of pelvis motion in the pattern with the minimum RCOF are less than those with the maximum SM. Also, since vertical acceleration affects ZMP, in order to have motion with the maximum SM, this component may be used. That is why fluctuation of vertical component of the pelvis trajectory in this motion is more than that with the minimum RCOF. Furthermore, in Fig. 9, the ZMP trajectories in both sagittal and lateral directions are illustrated. As it can be seen, while the ZMP trajectories for both cases are within SP, which shows the tip-over stability of the obtained gaits, for the pattern with the minimum RCOF, the ZMP trajectory is closer to the SP margins. In fact, in order to have the motion with less

https://doi.org/10.1017/S0263574715000715 Published online by Cambridge University Press

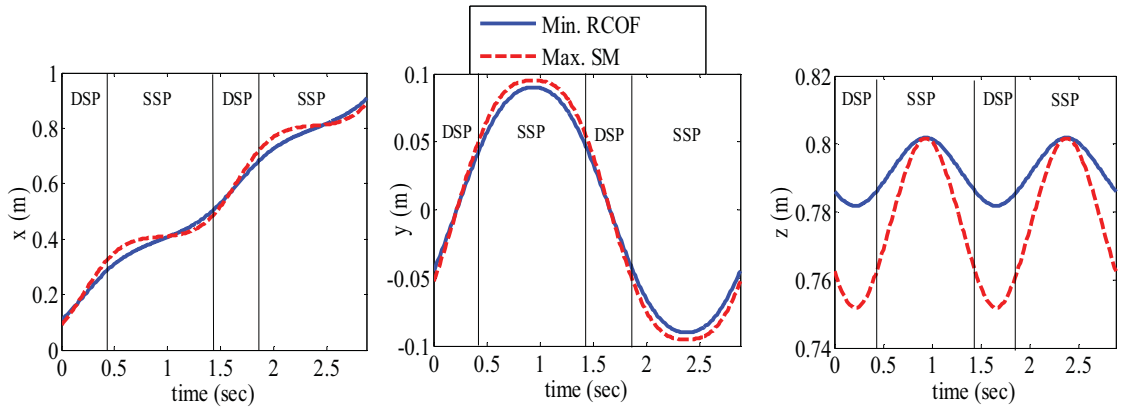


Fig. 8. Pelvis trajectory during one gait cycle.

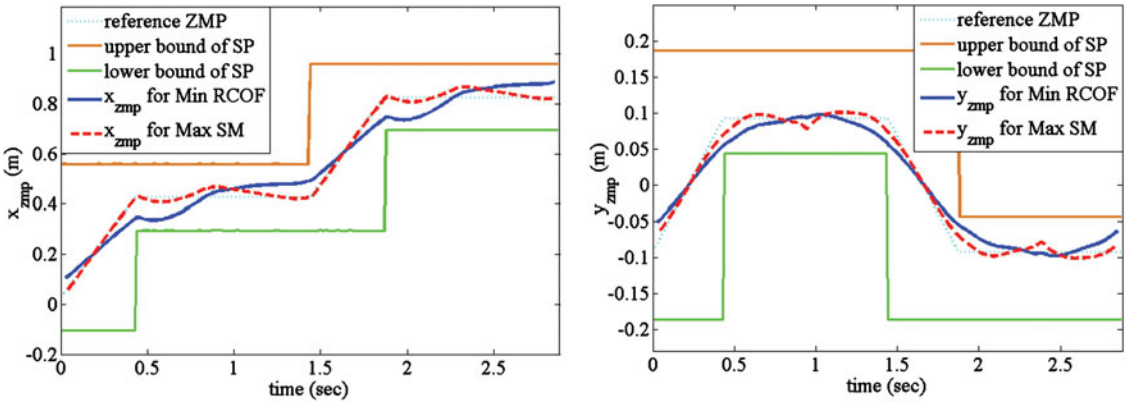


Fig. 9. ZMP trajectory for sagittal and lateral directions during one gait cycle.

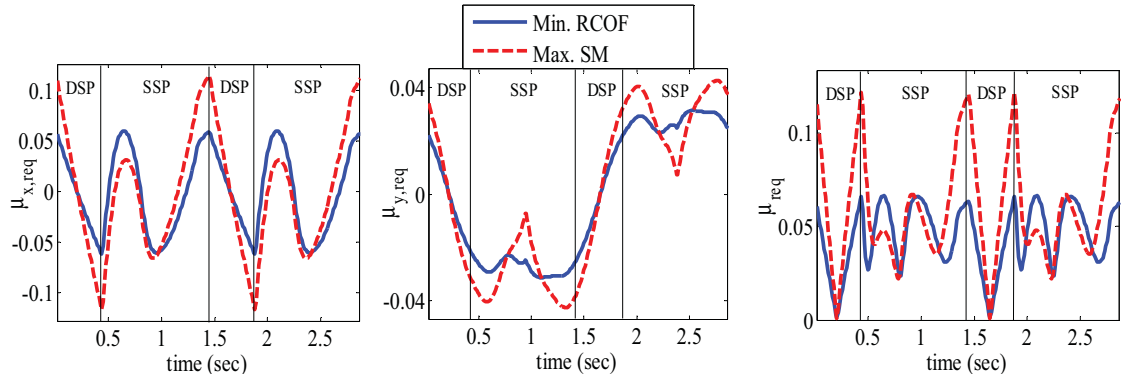


Fig. 10. Time history of RCOF during one gait cycle.

RCOF, the SM should be reduced. So, in order to generate walking pattern with a specified velocity, a compromise between SM and RCOF should be made. To be more specific, the results relate that for walking on slippery surfaces, the constraint of being ZMP in the middle of SP should be relaxed. This would alleviate fluctuations of the upper-body motion, which causes reduction in RCOF.

In order to investigate possibility of slipping in the sagittal and lateral directions, $\mu_{x,\text{req}}$ and $\mu_{y,\text{req}}$ as RCOF in the sagittal and lateral directions are plotted in Fig. 10. As it can be observed from these figures, for the speed of 1 Km/h, RCOF in the sagittal direction is greater than RCOF in the lateral direction. So, the robot has tendency to slip forward or backward more than sideward. Furthermore, time history of $\mu_{x,\text{req}}$ shows that the robot has tendency to slip forward at the beginning ($\mu_{x,\text{req}}$ has

https://doi.org/10.1017/S0263574715000715 Published online by Cambridge University Press

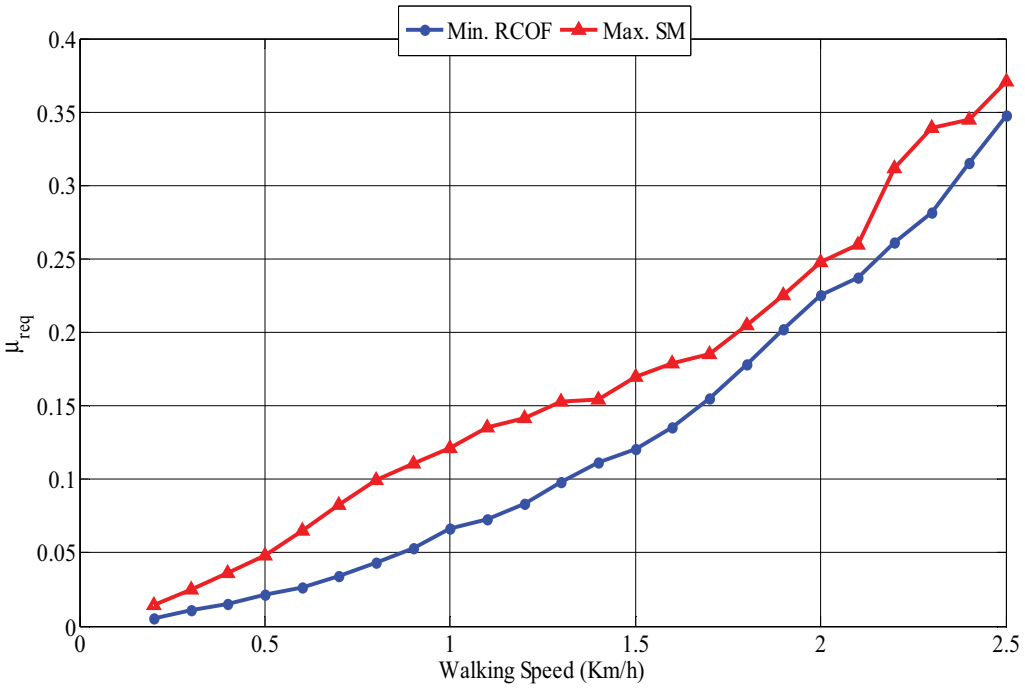


Fig. 11. Minimum RCOF for walking with various walking speeds.

negative value), and slip backward at the end ($\mu_{x,\text{req}}$ has positive value) of SSP which is consistent with the results reported for human walking.[21] Also, as it can be seen from time history of μ_{req}, the possibility of slipping for the pattern with the minimum RCOF is almost half of the one with the maximum SM. This means by employing suitable pelvis trajectory, the risk of slippage for walking on slippery surfaces can be alleviated up to 50%. Referring to the biomechanical study on human walking, reducing RCOF in the case that human beings anticipate slippery condition is an effective strategy for reducing risk of slippage.[18,19,21]

Finally, to have an estimation of the coefficient of friction that the patterns would demand for various walking speeds, RCOF versus walking speed is illustrated in Fig. 11, for both the pattern with minimum RCOF and the one with maximum SM. More inspection on this figure reveals that for each walking speed, there exists a band between two patterns. This band suggests that whether the tip-over stability or slipping is more crucial, the walking pattern should approach to the motion with the maximum SM or the motion with the minimum RCOF. It should be noted that although the pattern that is obtained from the minimum RCOF method needs the lowest friction amongst all feasible motions, it can be found some feasible walking patterns that need more friction than the motion with the maximum SM. In fact, the patterns with the maximum SM are obtained to be exploited in the case that the tip-over stability is crucial and there is no concern about slipping. These optimal patterns introduce the walking patterns that may be employed by the high-level control unit, in critical situations. Also, it is noteworthy that the best option for walking with a specified speed and on a predefined terrain is the one that makes a compromise between SM and RCOF.

4.3. Parametrical study

In the procedure of optimization of the walking gaits, just the pelvis parameters have been considered as the design variables. So, in this subsection, the effects of the step length D_s, and the ratio of DSP time to step period $\left(\frac{T_d}{T_c}\right)$ on RCOF will be discussed.

In order to inspect effect of the step length on RCOF, for different values of D_s the optimization procedure is conducted to find the minimum RCOF. The results for walking speed of 1 Km/h are illustrated in Fig. 12. As it can be seen, by increasing the step length, μ_{req} decreases to a certain level and then increases. This observation suggests that for each walking speed, there exist a step length with which the maximum RCOF is a minimum. In fact, for each walking speed, there exist a step length which minimizes the fluctuation of the upper-body, while generate a feasible walking pattern.

https://doi.org/10.1017/S0263574715000715 Published online by Cambridge University Press

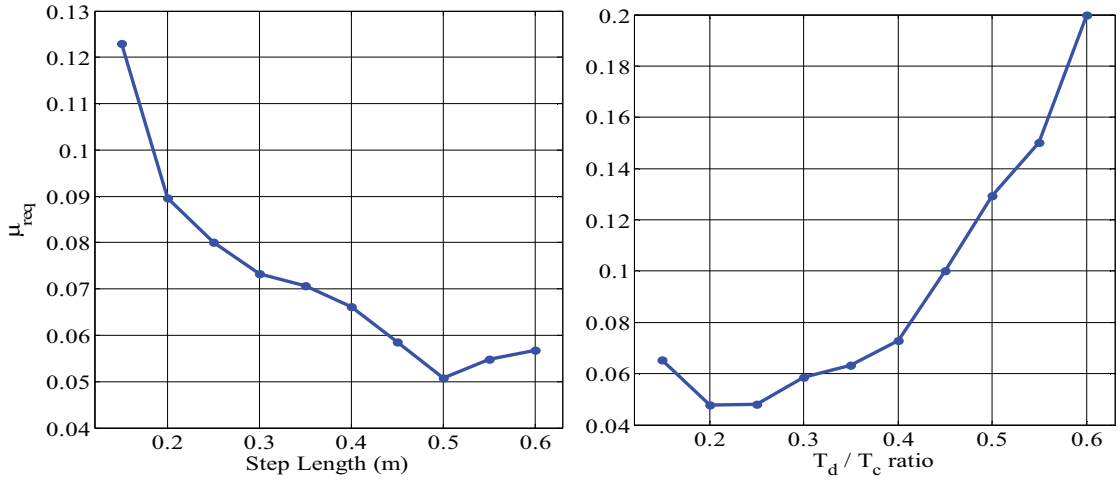


Fig. 12. Effects of step length ($\boldsymbol{D_s}$) and DSP time span to step period $\left(\frac{T_d}{T_c}\right)$ on RCOF.

This smooth upper-body motion demands low horizontal forces which means μ_{req} is a minimum. As it can be observed from Fig. 12, for walking pattern with the speed of 1 Km/h, the step length of 50 cm is the best option in terms of the minimum RCOF.

The other parameter that we would like to investigate its effect on RCOF is the ratio of the DSP time to the step period $\left(\frac{T_d}{T_c}\right)$. So, again the optimization procedure is conducted for different values of this ratio to find the trend of the changes of RCOF with respect to this ratio. As it can be concluded from Fig. 12, there exists a ratio with which RCOF is a minimum. The interesting point is that the optimum ratio is 0.2 that is the ratio which is consistent with human walking.[13]

5. Conclusions

In this article, a medium for optimal gait planning of humanoid robots on slippery surfaces was developed. In this medium, the optimization procedure for obtaining the motion with the minimum RCOF was conducted and compared to the one with the maximum tip-over SM. This comparison revealed that the band between RCOF of both approaches constitutes a spectrum of which two extremes yield the motion with the minimum RCOF and the maximum SM. Consequently, whether slipping or tipping-over is crucial, under a certain circumstance, the walking pattern should approach to the one with the minimum RCOF or the maximum SM. Furthermore, it was observed, for walking at 1 Km/h, that the robot has tendency to slip forward or backward more than sideward. Besides, parametrical studies on the step length, and the DSP to step period ratio revealed that by increasing these parameters, RCOF decreased first and then increased. This means for each motion speed, there exist a step length and a ratio that RCOF is a minimum. Finally, the experimental results verified the optimization results.

Acknowledgment

The authors would like to express deep gratitude to the Industrial Development and Renovation Organization of Iran (IDRO) for their financial supports to develop the robot SURENA III. We further thank to the members of CAST for their valuable participation in the design and fabrication of SURENA III humanoid robot.

References

1. P. Channon, S. Hopkins and D. Pham, "Derivation of optimal walking motions for a bipedal walking robot," *Robotica* **10**(02), 165–172 (1992).
2. C. Chevallereau and Y. Aoustin, "Optimal reference trajectories for walking and running of a biped robot," *Robotica* **19**(05), 557–569 (2001).

https://doi.org/10.1017/S0263574715000715 Published online by Cambridge University Press

3. M. Rostami and G. Bessonnet, "Sagittal gait of a biped robot during the single support phase. Part 2: Optimal motion," *Robotica* **19**(03), 241–253 (2001).
4. G. Bessonnet, P. Seguin and P. Sardain, "A parametric optimization approach to walking pattern synthesis," *Int. J. Robot. Res.* **24**(7), 523–536 (2005).
5. M. J. Sadigh and S. Mansouri, "Application of phase-plane method in generating minimum time solution for stable walking of biped robot with specified pattern of Motion," *Robotica* **31**(06), 837–851 (2013).
6. A. Goswami, "Postural stability of biped robots and the foot-rotation indicator (FRI) point," *Int. J. Robot. Res.* **18**(6), 523–533 (1999).
7. M. B. Popovic, A. Goswami and H. Herr, "Ground reference points in legged locomotion: Definitions, biological trajectories and control implications," *Int. J. Robot. Res.* **24**(12), 1013–1032 (2005).
8. M. Vukobratović and J. Stepanenko, "Mathematical models of general anthropomorphic systems," *Math. Biosci.* **17**(3), 191–242 (1973).
9. M. Vukobratović and B. Borovac, "Zero-moment point—-thirty five years of its life," *Int. J. Humanoid Robot.* **1**(01), 157–173 (2004).
10. S. Kajita, F. Kanehiro, K. Kaneko, K. Fujiwara, K. Harada, K. Yokoi and H. Hirukawa, "Biped Walking Pattern Generation by using Preview Control of Zero-moment Point," *Proceedings of the ICRA'03, IEEE International Conference on. Robotics and Automation*, (IEEE, 2003) pp. 1620–1626.
11. S. Kajita, F. Kanehiro, K. Kaneko, K. Fujiwara, K. Yokoi and H. Hirukawa, "Biped walking pattern generation by a simple three-dimensional inverted pendulum model," *Adv. Robot.* **17**(2), 131–147 (2003).
12. S. Kagami, T. Kitagawa, K. Nishiwaki, T. Sugihara, M. Inaba and H. Inoue, "A fast dynamically equilibrated walking trajectory generation method of humanoid robot," *Auton. Robots* **12**(1), 71–82 (2002).
13. Q. Huang, K. Yokoi, S. Kajita, K. Kaneko, H. Arai, N. Koyachi and K. Tanie, "Planning walking patterns for a biped robot," *IEEE Trans. Robot. Autom.* **17**(3), 280–289 (2001).
14. V.-H. Dau, C.-M. Chew and A.-N. Poo, "Achieving energy-efficient bipedal walking trajectory through GA-based optimization of key parameters," *Int. J. Humanoid Robot.* **6**(04), 609–629 (2009).
15. G. Capi, Y. Nasu, L. Barolli, K. Mitobe and K. Takeda, "Application of genetic algorithms for biped robot gait synthesis optimization during walking and going up-stairs," *Adv. Robot.* **15**(6), 675–694 (2001).
16. J. H. Park and M. Choi, "Generation of an optimal gait trajectory for biped robots using a genetic algorithm," *JSME Int. J. Ser.* C **47**(2), 715–721 (2004).
17. A. J. Chambers, S. Perera and R. Cham, "Changes in walking characteristics of young and older adults when anticipating slippery floors," *IIE Trans. Occup. Ergon. Hum. Factors* **1**(3), 166–175 (2013).
18. A. R. Oates, J. S. Frank and A. E. Patla, "Control of dynamic stability during adaptation to gait termination on a slippery surface," *Exp. Brain Res.* **201**(1), 47–57 (2010).
19. D. T.-P. Fong, Y. Hong and J.-X. Li, "Human walks carefully when the ground dynamic coefficient of friction drops below 0.41," *Saf. Sci.* **47**(10), 1429–1433 (2009).
20. R. C. Cooper, L. M. Prebeau-Menezes, M. T. Butcher and J. E. Bertram, "Step length and required friction in walking," *Gait & Posture* **27**(4), 547–551 (2008).
21. H. Nagano, W. Sparrow and R. K. Begg, "Biomechanical characteristics of slipping during unconstrained walking, turning, gait initiation and termination," *Ergonomics* **56**(6), 1038–1048 (2013).
22. W.-R. Chang, M. F. Lesch, C.-C. Chang and S. Matz, "Contribution of gait parameters and available coefficient of friction to perceptions of slipperiness," *Gait & Posture* **41**(1), 288–290 (2015).
23. W.-R. Chang, C.-C. Chang and S. Matz, "Comparison of different methods to extract the required coefficient of friction for level walking," *Ergonomics* **55**(3), 308–315 (2012).
24. H. Yamamoto and K. Ohnishi, "An Approach to Stable Walking on unknown Slippery Floor for Biped Robot," *The 27th Annual Conference of the IEEE. Industrial Electronics Society*, (IEEE, 2001) pp. 1728–1733.
25. K. Kaneko, F. Kanehiro, S. Kajita, M. Morisawa, K. Fujiwara, K. Harada and H. Hirukawa, "Slip Observer for Walking on a Low Friction Floor," *IEEE/RSJ International Conference on Intelligent Robots and Systems*, (IEEE, 2005) pp. 634–640.
26. I. Hashlamon and K. Erbatur, "Ground Reaction Force Sensor Fault Detection and Recovery Method based on Virtual Force Sensor for walking Biped Robots," *9th Asian. Control Conference (ASCC)*, (IEEE, 2013) pp. 1–6.
27. S. Roosen, "Ground-Contact Friction Estimation and Slip Prevention in Bipedal Robots," *Master Thesis*, (University of Melbourne, Department of Mechanical Engineering, 2012).
28. P. Bliman and M. Sorine, "Easy-to-use Realistic Dry Friction Models for Automatic Control," *Proceedings of 3rd European Control Conference*, Rome, Italy, (1995) pp. 3788–3794.
29. X. Zhou, Y. Guan, L. Jiang, H. Zhu, C. Cai, W. Wu and H. Zhang, "Stability of biped robotic walking with frictional constraints," *Robotica* **31**(04), 573–588 (2013).
30. T. Hirabayashi, B. Ugurlu, A. Kawamura and C. Zhu, "Yaw Moment Compensation of Biped Fast Walking using 3D Inverted Pendulum," *AMC'08. 10th IEEE International Workshop on. Advanced Motion Control* (IEEE, 2008) pp. 296–300.
31. B. Ugurlu, J. A. Saglia, N. G. Tsagarakis and D. G. Caldwell, "Yaw moment compensation for bipedal robots via intrinsic angular momentum constraint," *Int. J. Humanoid Robot.* **9**(04), (2012).
32. S. Kajita, K. Kaneko, K. Harada, F. Kanehiro, K. Fujiwara and H. Hirukawa, "Biped walking on a Low Friction Floor," *Proceedings of the IEEE/RSJ International Conference on Intelligent Robots and Systems,* (IEEE, 2004) pp. 3546–3552.

https://doi.org/10.1017/S0263574715000715 Published online by Cambridge University Press

33. M. Brandao, K. Hashimoto, J. Santos-Victor and A. Takanishi, "Gait planning for biped locomotion on slippery terrain," **In**: *14th IEEE-RAS International Conference on, Humanoid Robots* (IEEE, 2014), pp. 303–308.
34. G. N. Boone and J. K. Hodgins, "Slipping and tripping reflexes for bipedal robots," *Auton. Robots* **4**(3), 259–271 (1997).
35. O. Kwon and J. H. Park, "Reflex control of bipedal locomotion on a slippery surface," *Adv. Robot.* **16**(8), 721–734 (2002).
36. M. Khadiv, S. Ali A. Moosavian and M. Sadedel, "Dynamics Modeling of Fully-Actuated Humanoids with General Robot-Environment Interaction," *International Conference on Robotics and Mechatronics (ICROM)*, Tehran, Iran (IEEE, 2014).
37. H. A. Park, M. A. Ali and C. G. Lee, "Closed-form inverse kinematic position solution for humanoid robots," *Int. J. Humanoid Robot.* **9**(03), (2012).
38. M. Khadiv and S. Ali A. Moosavian, "A low friction demanding approach in gait planning for humanoid robots during 3D manoeuvres," *J. Appl. Mech.* **45**(1), 47–60 (2014).

https://doi.org/10.1017/S0263574715000715 Published online by Cambridge University Press